Development and Evaluation of a Model for Liquid-based Photovoltaic/Thermal Panels in TRNSYS

Kristen Jaczko[1], Stephen Harrison[2]
[1]Sustainability and Energy, Buildings, WSP, Toronto Ontario, Canada
[2]Solar Calorimetry Laboratory, Department of Mechanical and Materials Engineering
Queen's University, Kingston Ontario, Canada

Abstract

Photovoltaic/thermal (PV/T) collectors combine features of a solar thermal collector and a PV module into a single panel to maximize the collection of thermal and electrical energy. There currently are several simulation models in TRNSYS for PV/T modules, however, these are for PV/T panels cooled by circulating a fluid though an integral "tube and sheet" absorber (i.e., heat exchanger) and are not suitable for a large group of commercially available PV/T panels that incorporate a "fully wetted" absorber bonded to the back side of a conventional PV panel. The existing PV/T models in TRNSYS are also not suitable for simulating the performance of a panel when the surround ambient temperature is higher than the inlet fluid temperature, and as such, a new PV/T model was developed and implemented. This model iteratively solves for the panel's outlet fluid temperature and estimates the PV power output under specified conditions. This paper describes the theoretical basis of the new model and compares the simulated and experimental data. To test the new model, simulation results were compared to data experimentally measured on an operating PV/T array. These results indicate that the new TRNSYS model was able to predict the performance of the PV/T panel to within the estimated measurement error.

Introduction

Several different numerical models for PV/T panels have been developed since this concept first emerged. Florschuetz (1979) developed an extension to the Hottel-Whillier model of flat plat thermal collectors to predict the performance of a sheet-and-tube PV/T panel. The model used a modified collector heat removal factor $(\tilde{F}_R)$, modified collector efficiency factor $(\tilde{F}')$, modified overall collector heat loss coefficient $(\tilde{U}_L)$, and modified solar radiation $(\tilde{S})$ to calculate the production of electrical and thermal energy. Eq.'s 1 and 2, below, were used to calculate the energy production of the PV/T panel (Florschuetz, 1979).

$$\dot{Q}_e = \frac{A_c S \eta_{elec,amb}}{\alpha}\left[1-\frac{\eta_{elec,ref}\beta_r}{\eta_{elec,amb}}\ldots \ldots\left(\tilde{F}_R\left(T_i-T_{amb}\right)+\frac{\tilde{S}}{\tilde{U}_L}\left(1-\tilde{F}_R\right)\right)\right] \quad (1)$$

$$\tilde{Q}_{th} = A_c \tilde{F}_R\left[\tilde{S}-\tilde{U}_L\left(T_i-T_{amb}\right)\right] \quad (2)$$

Tiwari and Sodha (2006) created a theoretical model and compared the simulated value of daily thermal efficiency of the PV/T panel to the experimental results found by Huang *et al.,* (2001). A cross-sectional view of the PV/T panel used by Huang *et al.,* (2001) and simulated by Tiwari and Sodha (2006) is shown in Figure 1.

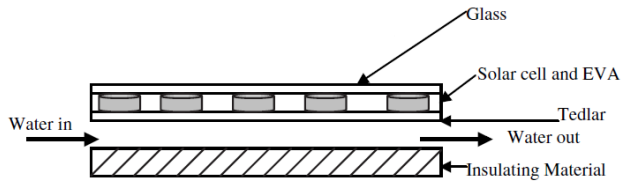

Figure 1: Schematic of PV/T module studied (Tiwari and Sodha, 2006).

The model was very similar to the Hottel-Whillier-Bliss equation of thermal efficiency but included two additional penalty factors; due to the solar cell material, tedlar, the two layers of ethylene vinyl acetate (EVA) that encapsulate the PV cells and glass cover (h_{P1}) and due to the interface between the tedlar and the working fluid (h_{P2}) (Eq. 3).

$$\eta_{th}^{*} = F_R\left[h_{P1}h_{P2}(\tau\alpha)-U_L\frac{T_i-T_{amb}}{I_T}\right] \quad (3)$$

The study predicted a daily efficiency of approximately 58% which showed good agreement of with results obtained by Huang *et al.,* (2001) under similar operating conditions (Tiwari and Sodha, 2006).

A review of the current PV/T models in TRNSYS was also performed as part of the International Energy Agency's Solar Heating and Cooling Programme Task 35 "PV/Thermal Solar Systems", The review looked three TRNSYS component models (Type 50, 555 and Type 56(0, 3, 6, 7, 8, 9)) as well as other TRNSYS models that had been independently developed. It was noted that the Type 50 model had eight operational modes but contained several errors that limited its usability. Type 555 was specifically designed for an unglazed air collector and Type 56(0, 3, 6, 7, 8, 9) was only applicable for systems where the collector was integrated into the building.

As a result of these limitations, a number of new generic TRNSYS components were developed, including;

- Type 201 for transpired PV/T air collectors,
- Type 250 for modelling of glazed and unglazed flat plat PV/T collectors using any fluid, and,
- Type 251 for concentrating PV/T collectors.

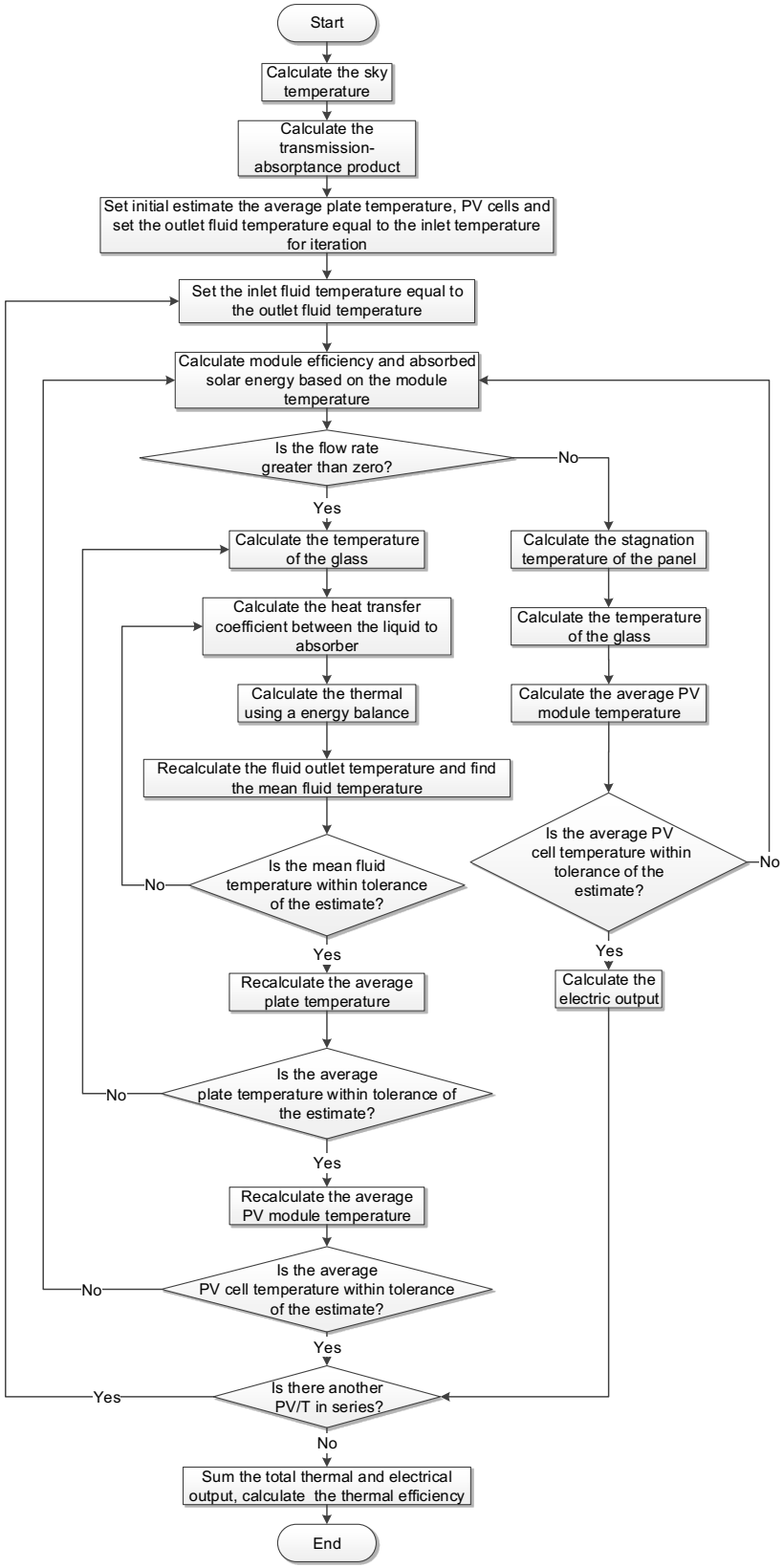

Figure 2: Flow chart demonstrating the process of Type 348 (Jaczko, 2017).

Type 250 is applicable for simulating fully wetted PV/T panels, however the model does not account for heat transfer from the ambient surroundings to the collector in cases when the collector surface temperature is lower than the surround air temperature (Collins, 2009) such as the case of a PV/T panel cooled by a heat pump to temperatures below the surrounding ambient temperature.

In the present study, the model for a fully wetted flat plate thermal collector was modified to include the collection of electrical energy and to allow operation at panel temperatures below the ambient air temperature (even with zero solar irradiance). To investigate the accuracy of the new model, the performance of a commercially available PV/T collector was measured over a range of operating conditions and compared to the new model's predicted performance under similar conditions. The new model was designated Type 348.

Modelling Approach

A PV/T model, Type 348, was created based on a previously developed model of a flat-plate solar thermal collector (Harrison 2017). The simulation starts by guessing the initial outlet fluid temperature, average absorber plate temperature and PV cell temperature. Using these values, the one-dimensional heat transfer between the collector fluid, the absorber plate, the PV cells, the glass cover and the surroundings is calculated. Type 348 then recalculates the temperatures that were guessed at the start and iteratively finds the performance of the PV/T collector. If multiple panels are connected in series the inlet temperature of the next panel is set to the outlet temperature of the previous panel and the total thermal and electrical power outputs are found for each time step of the main system simulation. Figure 2 illustrates the process of determining the performance of the panel in the TRNSYS subroutine.

Type 348 relies on linear factors relating the efficiency of the PV cells to the cell temperature and it is assumed that the PV module is always operating at its maximum power-point. The thermal portion of the model was based on an unglazed collector and applied an energy balance on the absorber plate, (Eq. 4), to determine the rate of thermal energy collection ($\dot{Q}_u$),

$$\dot{S} \cdot A_P = \dot{Q}_u + U_{Back} \cdot A_{back} \cdot \left(T_{plate,\,ave} - T_{amb,\,back}\right) \ldots \\ \ldots + \frac{A_P \cdot \left(T_{plate,\,ave} - T_{cover,\,ave}\right)}{R_{plate-to-cover}} \quad (4)$$

where A_p and A_{back} represent the aperture area and the back of the collector area respectively in m^2, U_{back} where A_p and A_{back} represent the aperture area and the back of the collector area respectively in m^2, U_{back} represents the heat loss coefficient of the absorber plate to the ambient air behind the collector W/(m^2·K), $R_{plate\text{-}to\text{-}cover}$ represents the thermal resistance of the encapsulant material between the absorber plate and the glass bonded to the PV cells in (m^2·K)/W, T_{plate}, $T_{amb,\ back}$ and $T_{cover,\ ave}$ represent the absorber plate temperature and ambient temperature behind the collector and the surface temperature of the glass, respectively in K. $\dot{S}$ is the net absorbed solar radiation and accounts for the radiation absorbed by the PV cells (i.e., Eq. 5) in W/m^2, i.e.,

$$\dot{S} = \dot{G} \cdot \left(\tau\alpha\right)_e \cdot \left(1 - \eta_{PV,e}\right) \quad (5)$$

where $\dot{G}$ represents the solar radiation incident on the collector surface in W/m^2, $(\tau\alpha)_e$ represents the effective transmission-absorption product of the collector, and $\eta_{PV,\ e}$ represents the actual efficiency of the PV module at the current temperature.

As previously mentioned, the efficiency of the PV module depends on the temperature of the cells (T_{PV}) and the packing factor (PF) of the cells on the panel (Eq. 6),

$$\eta_{PV,\,e} = \eta_{PV,\,ref} \cdot PF \cdot \left(1 - \beta_r \left(T_{PV} - T_{ref}\right)\right) \quad (6)$$

where β_r represents the temperature coefficient of the photovoltaic cells and T_{ref} is the reference temperature for the PV cells at the reference efficiency ($\eta_{PV,\ ref}$). The electrical power generated by the PV/T panel is calculated using Eq. 7.

$$\dot{Q}_{elec} = \dot{G} \cdot \left(\tau\alpha\right)_e \cdot A_p \cdot \eta_{PV,e} \quad (7)$$

The temperature of the glass cover is determined by iteratively solving the following equation,

$$\frac{\left(T_{cover,\,ave} - T_{plate,\,ave}\right)}{R_{plate-to-cover}} = h_w \cdot \left(T_{cover,\,ave} - T_{amb}\right) + \ldots \\ \ldots \varepsilon_{cover} \cdot \sigma \cdot \left(T^4_{cover,\,ave} - T^4_{amb}\right) \quad (8)$$

where h_w represents the convection heat transfer coefficient due to wind W/(m^2·K), ε_{cover} represents the emissivity of the glass cover, σ is the Stephan-Boltzmann constant i.e., $5.67 \cdot 10^{-8}$ W/(m^2·K^4). The thermal resistance between the absorber plate and the outer surface of the cover accounting for the EVA that encapsulate the PV cells and the resistance of the glass, is given by,

$$R_{plate-to-cover} = R_{EVA} + R_{cover} = \frac{t_{EVA}}{k_{EVA}} + \frac{t_{cover}}{k_{cover}} \quad (9)$$

The convection coefficient across the top of the collector was calculated using the correlation from McAdams (1954),

$$h_w = 5.7 + 3.8 V_w \quad (10)$$

where V_w represent the wind speed in m/s (McAdams, 1954). As seen in Eq. 11, the fluid temperature at outlet of the collector, as well as the plate and PV average temperatures, are initially estimated and then recalculated using the value of the absorbed useful thermal energy, and the mean fluid temperature is then estimated by Eq. 12.

$$T_{fluid,\,outlet} = T_{fluid,\,inlet} + \frac{\dot{Q}_u}{\dot{m} \cdot c_p} \quad (11)$$

Table 1: Type 348 model parameters, inputs and outputs and if equivalents exist in Type 250.

Type 348 Parameters	Equivalent Type 250 Parameters	Type 348 Inputs	Equivalent Type 250 Inputs	Type 348 Output	Equivalent Type 250 Outputs
Gross Area of Collector	Yes	Fluid Inlet Temperature	Yes	Fluid Outlet Temperature	Yes
Aperture Area of Collector	No	Collector Flowrate	Yes	Average Cell Temperature	Yes
Back Area of Collector	No	Collector Slope	Yes	Thermal Output	Yes
Length of Absorber	No	Ambient Temperature	Yes	Electrical Output	Yes
Flow Channel Hydraulic Diameter	No	Incident Radiation	Yes	Thermal Efficiency	No
Flow Channel Wetted Perimeter	No	Diffuse Fraction of Radiation	Yes	Electrical Efficiency	No
Back Loss Coefficient	Yes	Inclination Angle	Yes	Tau-Alpha	Yes
EVA Layer Conductivity	No	Wind Speed	Yes		
EVA Layer Thickness	No	Temperature at The Back of Panel	No		
Glass KL Product	Yes	Ground Emissivity	No		
Glass Emissivity	No	Ground Reflectivity	No		
Glass Conductivity	No				
Glass Thickness	No				
Number of Collectors in Series	No				
PV Absorptivity	Yes				
PV Emissivity	Yes				
PV Efficiency	Yes				
PV Temperature Coefficient	Yes				
PV Reference Temperature	Yes				
PV Packing Factor	Yes				

$$T_{fluid,\,ave} = \frac{T_{fluid,\,inlet} + T_{fluid,\,outlet}}{2} \tag{12}$$

To estimate the average plate temperature, the Nusselt number for parallel plates and convection heat transfer coefficient were determined from,

$$Nu = 4.9 + \frac{0.0606 \cdot \left(\mathrm{Re} \cdot \mathrm{Pr} \cdot D_h / L\right)^{1.2}}{1 + 0.0909 \cdot \left(\mathrm{Re} \cdot \mathrm{Pr} \cdot D_h / L\right)^{0.7} \cdot \mathrm{Pr}^{0.17}} \tag{13}$$

$$h_{fluid} = Nu \cdot \frac{k_{fluid}}{D_h} \tag{14}$$

where *Re* and *Pr* are the Reynolds and Prandtl numbers, D_h represents the hydraulic diameter of the collector in m, *L* represents the length of the collector absorber channel in m and k_{fluid} represents the conductivity of the collector fluid W/(m·K) (Duffie and Beckman, 2013). Thus, the average absorber plate temperature is found by,

$$T_{plate,\,ave} = T_{fluid,\,ave} - \frac{\dot{Q}_u}{h_{fluid} \cdot P_{channel} \cdot L} \tag{15}$$

where $P_{channel}$ represented the perimeter of the collector fluid channel in m. Finally, the temperature of the PV module was found using Eq. 16.

$$T_{PV} = T_{fluid,\,ave} + \frac{R_{EVA}\left(T_{plate,\,ave} - T_{cover,\,ave}\right)}{R_{plate-to-cover}} \tag{16}$$

The average temperatures of the glass cover, the absorber plate, the collector and the PV module are all converted into absolute temperatures (i.e., degrees Kelvin) in the subroutine and are solved for iteratively.

Table 1 contains the TRNSYS model parameters, inputs and outputs for Type 348 and evaluates if equitant parameters are used by Type 250. The inputs and outputs are very similar to those for Type 250, however Type 348 includes the emissivity and reflectivity of ground while Type 250 assumes the temperature behind the panel is equal to the ambient temperature. Type 348 allows for iterations based on the number of panels connected in series as seen in Figure 2. Type 250 includes the collector efficiency factor as a parameter to calculate the thermal performance of the panel while Type 348 uses the dimensions of the flow channel and Eq.'s 13 and 14. The same PV module parameters are used in both models and both account for heat loss from the back of the panel. Type 250 does not account for interactions between the PV cells and the bonded glass layer and EVA layers and thus does not include the relevant parameters.

Figure 3: Photo of rear of PVT panel showing the heat exchanger bonded to the back surface of the PV module.

Figure 4: Photo of the PVT array used to evaluate the accuracy of the new TRNSYS Type 348.

Experimental Methodology

For this study, a commercially available, fully-wetted absorber plate design (manufactured by DualSun) was modelled. Two versions of the product are available, consisting of: conventional PV panels with plate heat exchangers bonded to the back of the panel to extract heat – the plate heat exchangers were not insulated from the ambient (Figure 3) and, conventional PV panels with plate heat exchangers bonded to the back of the panel to extract heat – the plate heat exchangers were insulated from the ambient in a manner similar that described by Zondag, et al. 2003 (DualSun, 2017).

The PV/T model was compared to experimental data of DualSun Wave PV/T collector without back insulation. The test apparatus used for this study consisted two parts; a thermal loop and an electrical loop. Local mains water was run through two DualSun Wave PV/T (Figure 4) collectors connected in series and the temperature at the inlet and outlet of the of the collector rig and the flow rate of the mains water were recorded. The PV panels of each collector were also connected in series and to a resistor bank that was set to the estimated maximum power point of the collectors. The voltage and amperage output of the PV/T panels was monitored. Two inclined pyranometers were used to measure the total and diffuse radiation incident on the PV/T array. The ambient temperature was monitored using a shaded and shielded thermocouple and the local wind speed in front of the panels was monitored using a weather station. All measurements, except for wind speed, were monitored every four seconds. Due to limitations of the weather station the wind speed was only recorded every twelve minutes. The PV/T array's performance was tested using the operating conditions in Table 2.

Results

To determine the accuracy of the new TRNSYS PV/T model, Type 348, a series of tests were performed on two commercially available fully wetted liquid PV/T panels as shown in Figure 4. Table 2 details the operation conditions under which the tests were performed. The total rate of collection is designated as "Qtotal", the rate of thermal energy collection is designated as "Q" and the rate of electrical energy collection is designated as "QPV" in Figures 6 and 10.

Figure 5 displays the rate at which thermal energy was collected during the test period on July 29th, 2017. The average percentage difference between the experimental and simulated collection rate was 2.60% or 35.4 W. The outdoor air temperature was above the inlet temperature of the collector fluid for the duration of the experiment.

Figure 6 shows the plot of the thermal and electrical energy collection rate predicted by Type 358 and the collection rates calculated from the experimental data for July 31st, 2017. The collector fluid was below the ambient temperature for the entire test. The average difference in the rate of thermal and electrical collection was 7.5% and 8.4%, which is within estimations of the error of the experimental data. It was also observed that Type 348 reacted more rapidly to changes in the

Table 2: Operating conditions used to evaluate the PV/T collector.

Test Date	Average Inlet Temperature (°C)	Average Flow Rate (kg/min)	Average Ambient Temperature (°C)	PV On/Off
July 29th, 2017	24.6	3.60	18.9	Off
July 31st, 2017	18.6	3.40	27.0	On
August 21st,2017	40.1	2.35	27.0	Off
August 23rd, 2017	37.9	2.33	23.3	On

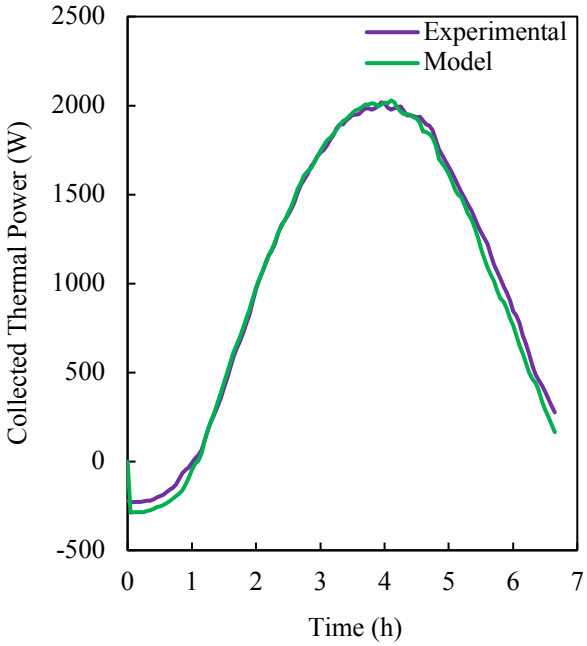

Figure 5: Experimental and model thermal collection rate of the DualSun PV/T panel on July 29th, 2017.

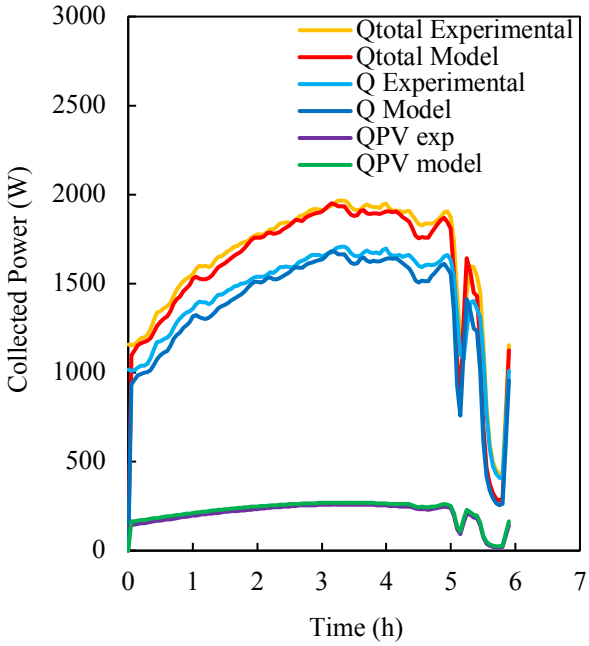

Figure 6: Experimental and model outputs of the DualSun PV/T panel on July 31st, 2017.

outdoor conditions. This is due to the model assuming that the PV/T panels do not have thermal capacity.

Figure 7 shows the outlet temperature of the PV/T panels for August 21st, 2017 obtained experimentally and from Type 348. The temperature of the collector fluid was above the ambient temperature for the duration of the test. Average difference of the predicted and experimental outlet temperatures was 0.91°C or a 2% difference. It is observed that the lack of thermal capacitance in the model results in a quicker reaction to changes in the conditions. The difference in the rate of thermal energy collection for August 21st, 2017 was 146.7 W and Figure 8 show the models rapid reaction to changes in operating conditions.

Figures 9 and 10 show the results of the August 23rd test. The ambient air temperature was below the inlet fluid temperature for the duration of the test and the PV cells were connected. The average fraction of diffuse radiation was 0.442 and ranged during the testing period between 0.198 and 0.931. Figure 9 show the recorded and simulated collector fluid outlet temperatures. The average difference between the model and the

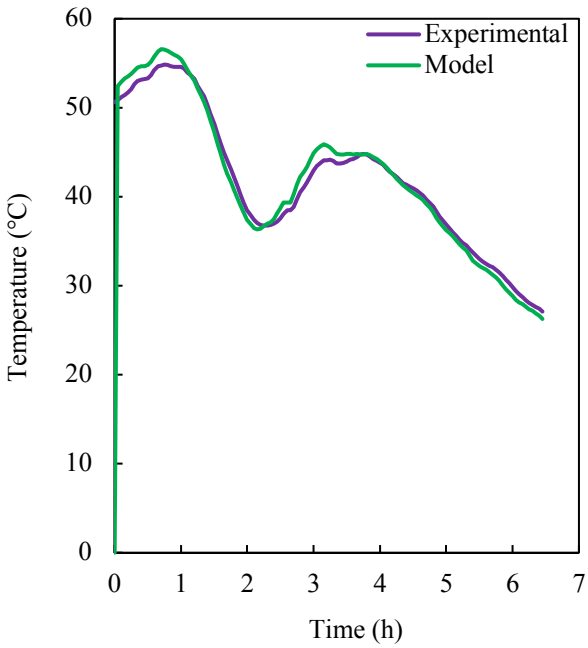

Figure 7: The experimental and predicted outlet fluid temperatures of the PV/T panels on August 21st, 2017.

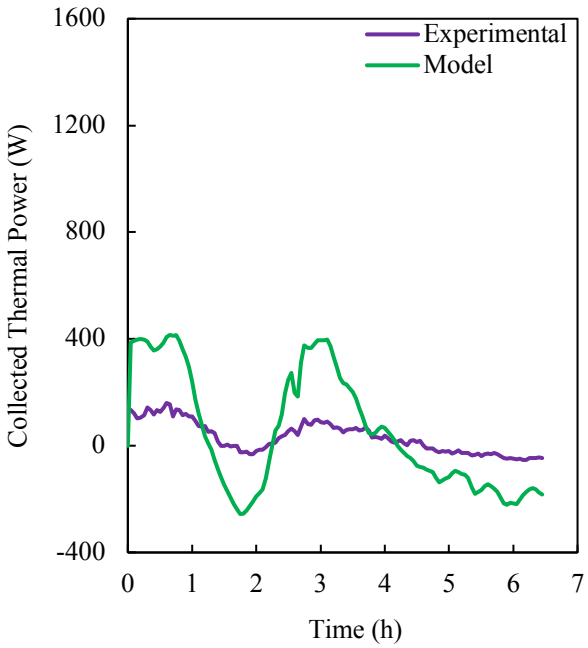

Figure 8: The experimental and predicted rates of thermal energy collection on August 21st, 2017.

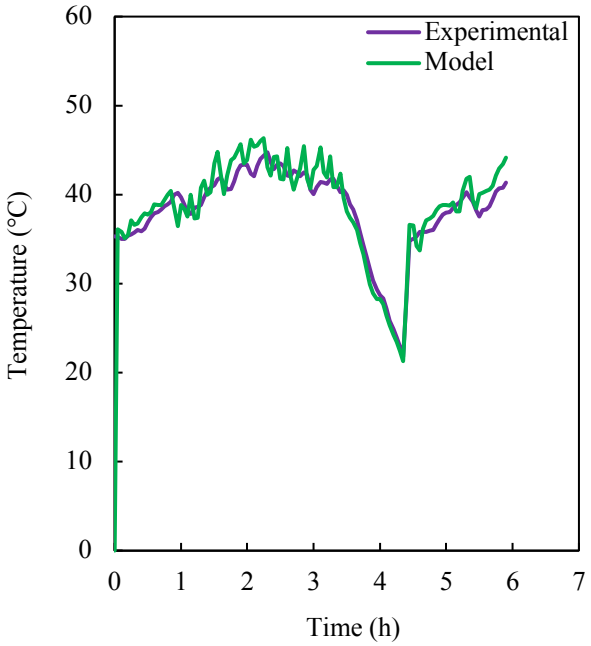

Figure 9: The experimental and predicted outlet fluid temperatures of the PV/T panels on August 23rd, 2017.

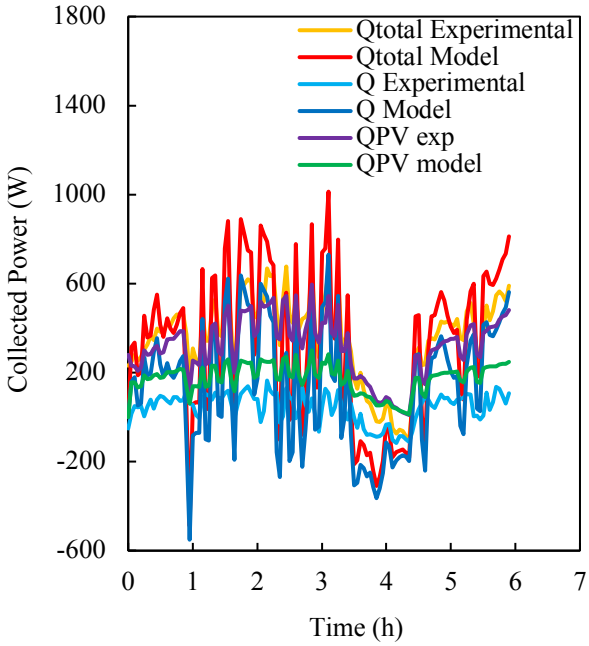

Figure 10: Experimental and model outputs of the DualSun PV/T panel on August 23rd, 2017.

experimental outlet temperature was 1.47°C. Figure 10 shows the total rate of thermal and electrical energy collection on August 23rd. The average difference between the experimental and predicted output was 172.5 W. This is within the experimental error for the apparatus.

Analysis

The experimental and simulation performance of the PV/T panels had very good agreement when the collector fluid inlet temperature was lower than the ambient air as seen in Figures 5 and 6. Figure 8 illustrates the impact of this lack of capacitance as the experimental thermal energy collected is very small and relatively constant for the entire test while the rate of the thermal energy collector predicted by Type 348 does vary with changes in outdoor conditions. Both the thermal and electrical performance were well within the range for the duration of the test. It was also observed that Type 348 reacted more rapidly to changes in the outdoor conditions as was seen in Figures 8 and 10 during fluctuating test conditions as the model is steady state. This issue was seen when the PV/T panels operate above the ambient temperature. The small difference in the outlet fluid temperature of the experimental and simulated results resulted in a much larger difference in thermal energy collection. This difference was still within the experimental error.

Conclusion

A new TRNSYS model of a fully wetted liquid photovoltaic/thermal collector that includes the absorption of ambient energy was developed. The model was used to compare the simulated and experimental performance of commercially available PV/T panels under a range of operating conditions.

The model showed very good agreement when tested with inlet temperatures above and below ambient temperature. As the model is steady-state, the simulated performance tended to react more rapidly to changes in temperature and incident radiation on the panel.

Acknowledgement

This research was supported by the Bert Wasmund Scholarship for Sustainable Energy Research and the ASHRAE Grant-in-Aid. The authors also wish to acknowledge the assistance of Gary Johnson and Denon Sheppard in setting up the apparatus.

Nomenclature

A	area [m^2]
c_p	specific heat [kJ/(kg·K)]
D	diameter [m]
F'	collector efficiency factor [-]
F_R	overall heat removal efficiency factor [-]
$\dot{G}$	incident solar radiation [W/m^2]
h	convective heat transfer coefficient [W/(m^2·K)]
k	conduction heat transfer coefficient [W/(m·K)]
L	length [m]
$\dot{m}$	mass flow rate [kg/s]
Nu	Nusselt number [-]
P	perimeter [m]
PF	packing factor [-]
Pr	Prandtl number [-]
$\dot{Q}$	rate of energy collection [W]
R	thermal resistance [(m^2·K)/W]

Re	Reynolds number [-]
$\dot{S}$	absorbed solar radiation [W/m^2]
T	temperature [°C, K]
U	heat loss coefficient [W/(m^2·K)]
UA	overall heat transfer coefficient [W/K]
V	wind speed [m/s]
α	absorptivity [-]
β_r	temperature coefficient of photovoltaic cells
ε	emissivity [-]
η	collector efficiency [%]
θ	incident angle [°]
σ	Stephan-Boltzmann constant [W/(m^2·K^4)]
τ	short-wave transmittance [-]
$(\tau\alpha)$	effective transmission-absorption product [-]

References

Armstrong, S., and W.G. Hurley. 2010. "A thermal model for photovoltaic panels under varying atmospheric conditions." *Applied Thermal Engineering* 30: 1488-95.

Calise, F., M.D. d'Accadia, R.D. Figaj, and L. Vanoli. 2016. "A novel solar-assisted heat pump driven by photovoltaic/thermal collectors: Dynamic simulation and thermoeconomic optimization." *Energy* 95: 346-66.

Collins, M. 2009. "A review of PV, solar thermal, and PV/thermal collector models in TRNSYS."

Collins, M., and H. Zondag. 2009. "Recomended standard for the characterization and monitoring of PV/Thermal Systems." IEA SHC - Task 35, Solar Heating and Cooling Programme International Energy Agency.

DualSun. 2017. *DualSun Wave.* https://dualsun.fr/wp-content/uploads/DualSun-EN-Datasheet.pdf.

Duffie, J A, and W A Beckman. 2013. *Solar Engineering of Thermal Processes.* Hoboken, New Jersey: John Wiley & Sons, Inc.

Florschuetz, L. W. 1979. "Extension of the hottel-whillier model to the analysis of combined photovoltaic/thermal flat plate collectors." *Solar Energy* 22: 361-66.

Harrison, S.J. 2017. "The potential and challenges of solar boosted heat pumps for domestic hot water heating." *12th IEA Heat Pump Conference.* Rotterdam, Netherlands.

Jaczko, K. 2017. "Integrated Energy System for a High Performance Building." MASc Thesis, Kingston, ON.

Lu, Z.H., and Q. Yao. 2007. "Energy analysis of si solar cell modules based on an optical model for arbitrary layers." *Solar Energy* 81: 636-47.

Matsukawa, H., and K. Kurokawa. 2005. "Temperature fluctuation analysis of photovoltaic models at short time interval." *31st IEEE Photovoltaic Specialists Conference.* 1816-9.

McAdams, W.H. 1954. *Heat Transmission.* 3rd. New York: McGraw-Hill.

Paradis, P.L., D.R. Rousse, L. Lamarche, and H. Nesreddine. 2017. "A 2-D transient numerical heat transfer model of the solar absorber plate to improve PV/T solar collector systems." *Solar Energy* 153: 366-378.

Santbergen, R., and R.J.C van Zolingen. 2008. "The absorption factor of crystalline silicon PV cells: A numerical and experimental study." *Solar Energy Materials & Solar Cells* 92 (4): 432-44.

Solimpeks Solar Energy Corp. 2017. *Volther Hybrid Collectors.* http://www.solimpeks.com/wp-content/uploads/2016/06/Volther-Datasheet-1.pdf.

Tiwari, A., and M. S. Sodha. 2006. "Performance evaluation of solar PV/T system: An experimental validation." *Solar Energy* 80: 751-9.

Zondag, H.A., D.W. de Vries, W.G.J. van Helden, and R.J.C. van Zolingen. 2003. "The yield of different combined PV-thermal collector designs." *Solar Energy* 74: 253-69.